Electronic Supplementary Material (ESI) for Journal of Materials Chemistry A.

Supporting Information

High Humidity-Resistive Triboelectric Nanogenerator via Coupling of Dielectric Materials Selection and Surface-Charge Engineering

Lu Liu,[a,b] Linglin Zhou,[a,b] Chuguo Zhang,[a,b] Zhihao Zhao,[a,b] Shaoxin Li,[a,b] Xinyuan Li,[a,b] Xing Yin,[a,b] Jie Wang*[a,b,c] and Zhong Lin Wang*[a,b,d]

[a] Beijing Institute of Nanoenergy and Nanosystems, Chinese Academy of Sciences, Beijing 101400, P. R. China

[b] School of Nanoscience and Technology, University of Chinese Academy of Sciences, Beijing 100049, P. R. China

[c.] School of Chemistry and Chemical Engineering, Center on Nanoenergy Research, Guangxi University, Nanning 530004, P. R. China

[d.] School of Materials Science and Engineering, Georgia Institute of Technology, Atlanta, GA 30332, USA

*Corresponding Author: J. Wang: wangjie@binn.cas.cn; Z. L. Wang: zhong.wang@mse.gatech.edu

Supporting Figures

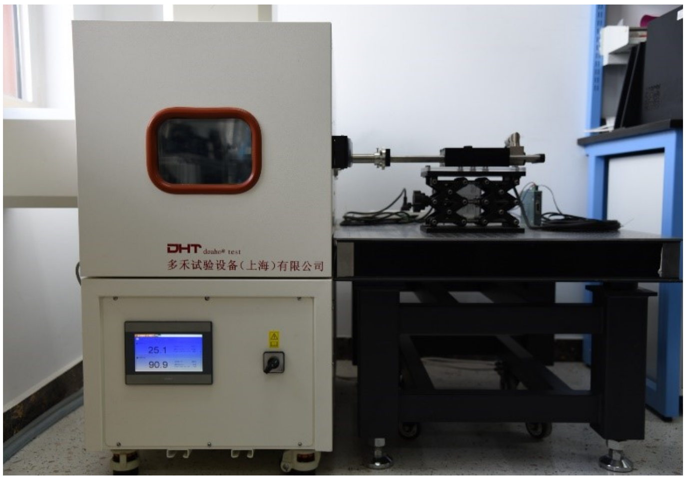

Fig. S1 Photograph of the measurement system.

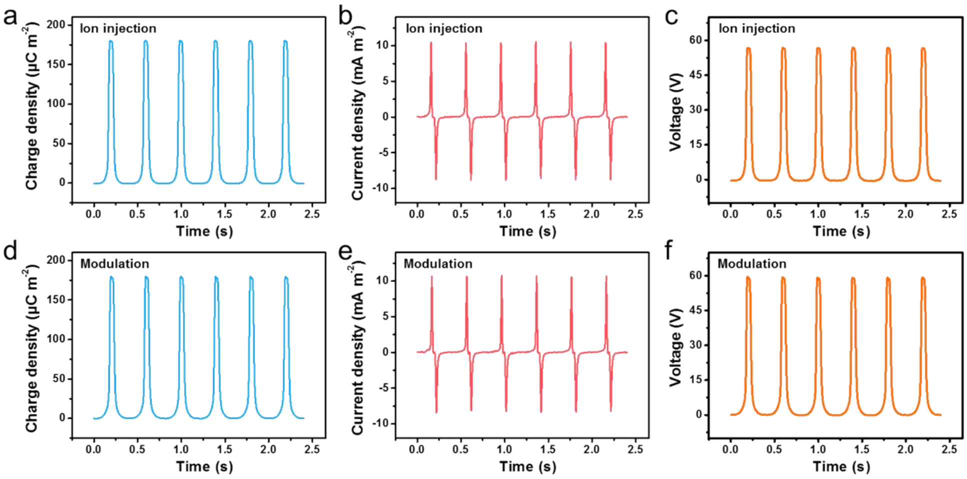

Fig. S2 Output performance of TENG through ion injection and modulation method. a) Charge density, b) current density and c) open-circuit voltage of the TENG device after ion injection applied on the PTFE film with a thickness of 100 μm. a) Charge density, b) current density and c) open-circuit voltage of the TENG device after modulation applied on the PTFE film with a thickness of 100 μm.

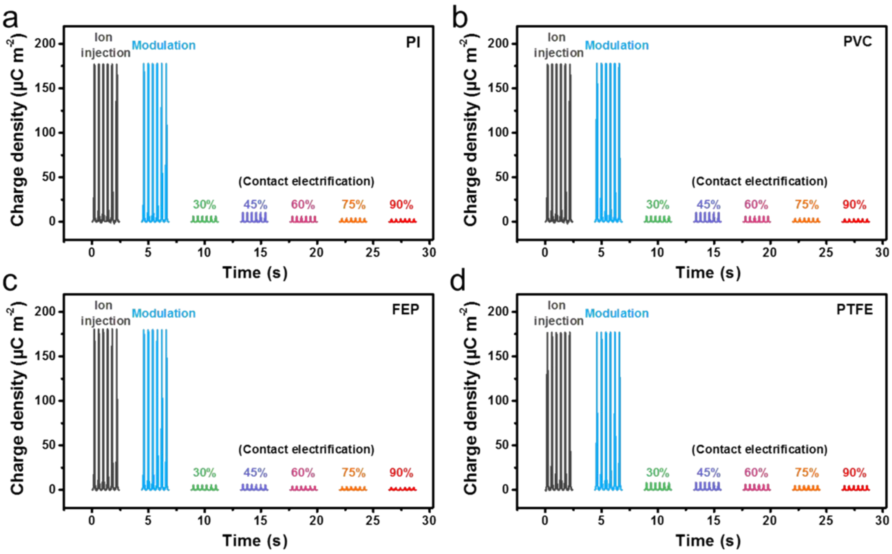

Fig. S3 The charge density on the a) PI, b) PVC, c) FEP, and d) PTFE surfaces generated by ion injection, modulation and contact electrification strategy.

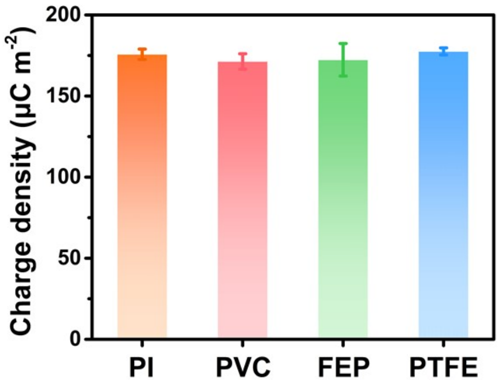

Fig. S4 Initial charge density on the PI, PVC, FEP, and PTFE surfaces introduced through ion injection.

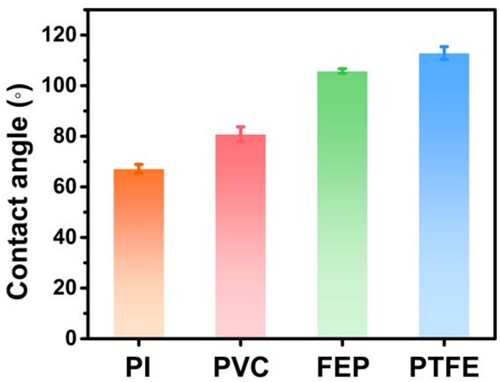

Fig. S5 The contact angles of PI, PVC, FEP, and PTFE surfaces.

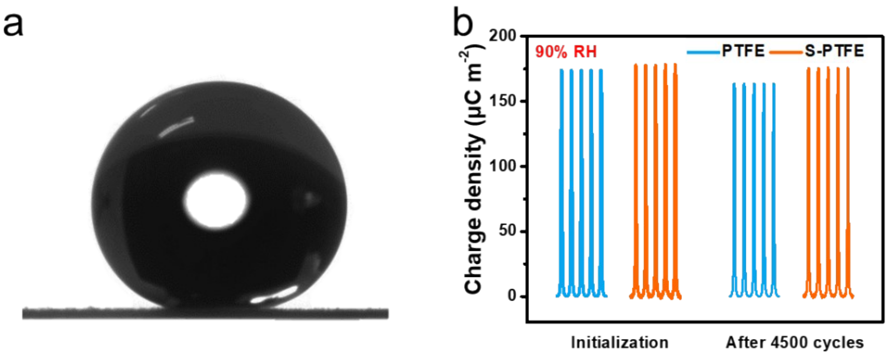

Fig. S6 The performance comparison of PTFE and S-PTFE film based TENG under high humidity environment. a) The water contact angle of S-PTFE film. b) The residual surface charges of PTFE and S-PTFE film before and after 4500 cycles continuous operation under 90% RH.

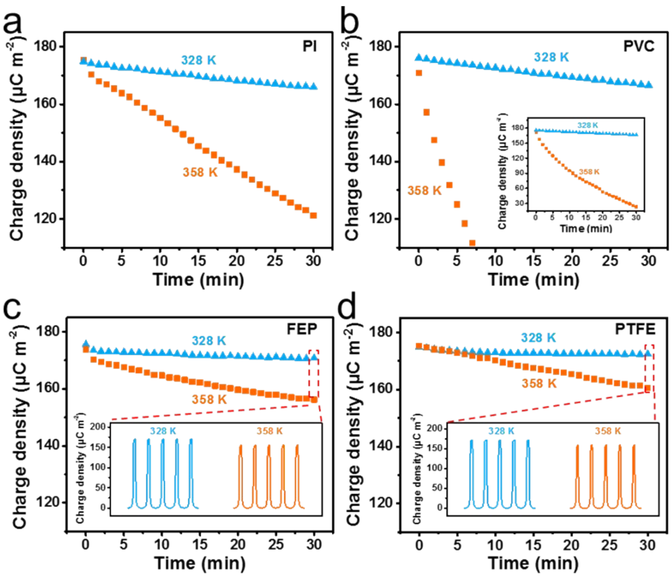

Fig. S7 Effect of temperature on the surface charges. The charge decay on the a) PI, b) PVC, c) FEP, and d) PTFE surfaces under different temperatures.

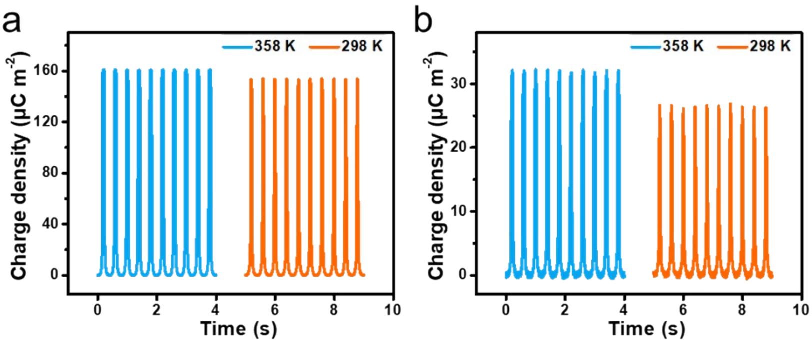

Fig. S8 The charge density introduced through ion injection and modulation approach on the PTFE surface when the temperature drops back to 298 K.

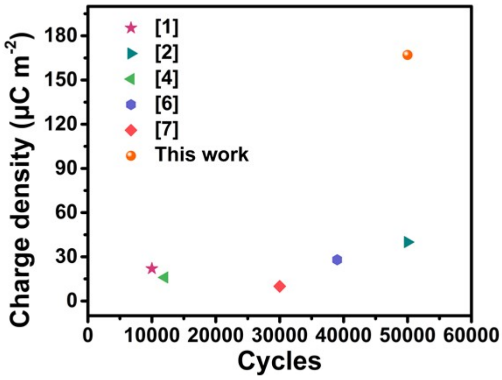

Fig. S9 Comparisons of the output performance of reported high humidity-resistive TENG.

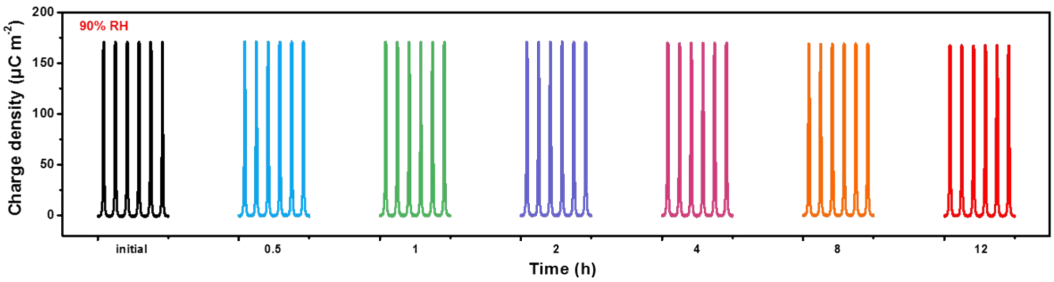

Fig. S10 Stability test of the TENG device based on ion-injected PTFE film in 90% RH over 12 hours.

Supplementary Notes

Note S1. Calculation of the equivalent charging current.

The equivalent charging current (I_{ec}) is calculated by the following equation:

$$I_{ec} = C \times \Delta V / \Delta t \tag{1}$$

where C denotes the capacitance of the capacitor, and ΔV denotes the voltage change of the capacitor during the charging/discharging time (Δt).

Supplementary Tables

Table S1. Comparisons of the output performance of TENG based on the ion-injected PTFE film with the previous classic works.

Type of TENG	Surface charge density	Relative humidity	Output stability	References
Fluorinated polymer sponge based TENG	22 μC m^{-2}	85%	10, 000 cycles	1
Hydrophobic ionic liquid gel based TENG	40 μC m^{-2}	80%	50, 000 cycles	2
Porous wood based TENG	10 μC m^{-2}	75%	/	3
Nanofibrous membranes based TENG	16 μC m^{-2}	90%	12, 000 cycles	4
Encapsulated porous cellulose based TENG	/	80%	10, 800 cycles	5
Starch films based TENG	28 μC m^{-2}	95%	39, 000 cycles	6
Cellulose Based TENG	10 μC m^{-2}	84%	30, 900 cycles	7
Packed TENG	22 μC m^{-2}	90%	/	8
Textile based TENG	42 μC m^{-2}	80%	/	9
Cellulose nanofibrils based TENG	/	90%	10, 000 cycles	10
Ion-injected PTFE film based TENG	167 μC m^{-2}	90%	50, 000 cycles	This work

References

1. Z. Peng, J. Song, Y. Gao, J. Liu, C. Lee, G. Chen, Z. Wang, J. Chen and M. K. H. Leung, *Nano Energy*, 2021, **85**, 106021.

2. P. Lv, L. Shi, C. Fan, Y. Gao, A. Yang, X. Wang, S. Ding and M. Rong, *ACS Appl. Mater. Interfaces*, 2020, **12**, 15012-15022

3. C. Cai, J. Mo, Y. Lu, N. Zhang, Z. Wu, S. Wang and S. Nie, *Nano Energy*, 2021, **83**, 105833.

4. J. Shen, Z. Li, J. Yu and B. Ding, *Nano Energy*, 2017, **40**, 282-288.

5. S. Adonijah Graham, B. Dudem, H. Patnam, A. R. Mule and J. S. Yu, *ACS Energy Lett.*, 2020, **5**, 2140-2148.

6. N. Wang, Y. Zheng, Y. Feng, F. Zhou and D. Wang, *Nano Energy*, 2020, **77**, 105088

7. R. Zhang, C. Dahlström, H. Zou, J. Jonzon, M. Hummelgård, J. Örtegren, N. Blomquist, Y. Yang, H. Andersson and M. Olsen, *Adv. Mater.*, 2020, **32**, 2002824.

8. A. Chandrasekhar, V. Vivekananthan, G. Khandelwal and S. J. Kim, *Nano Energy*, 2019, **60**, 850-856.

9. Y.-T. Jao, P.-K. Yang, C.-M. Chiu, Y.-J. Lin, S.-W. Chen, D. Choi and Z.-H. Lin, *Nano Energy*, 2018, **50**, 513-520.

10. S. Nie, Q. Fu, X. Lin, C. Zhang, Y. Lu and S. Wang, *Chem. Eng. J.*, 2021, **404**, 126512.